One-electron versus electron–electron interaction contributions to the spin–spin coupling mechanism in nuclear magnetic resonance spectroscopy: Analysis of basic electronic effects

Jürgen Gräfenstein and Dieter Cremer[a)]
Department of Theoretical Chemistry, Göteborg University, Reutersgatan 2, S-41320 Göteborg, Sweden

(Received 29 July 2004; accepted 8 October 2004)

For the first time, the nuclear magnetic resonance (NMR) spin–spin coupling mechanism is decomposed into one-electron and electron–electron interaction contributions to demonstrate that spin-information transport between different orbitals is not exclusively an electron-exchange phenomenon. This is done using coupled perturbed density-functional theory in conjunction with the recently developed J-**OC**-PSP [=J-OC-OC-PSP: Decomposition of J into *o*rbital *c*ontributions using *o*rbital *c*urrents and *p*artial *s*pin *p*olarization)] method. One-orbital contributions comprise Ramsey response and self-exchange effects and the two-orbital contributions describe first-order delocalization and steric exchange. The two-orbital effects can be characterized as external orbital, echo, and spin transport contributions. A relationship of these electronic effects to zeroth-order orbital theory is demonstrated and their sign and magnitude predicted using simple models and graphical representations of first order orbitals. In the case of methane the two NMR spin–spin coupling constants result from totally different Fermi contact coupling mechanisms. ^1J(C,H) is the result of the Ramsey response and the self-exchange of the bond orbital diminished by external first-order delocalization external one-orbital effects whereas ^2J(H,H) spin–spin coupling is almost exclusively mitigated by a two-orbital steric exchange effect. From this analysis, a series of prediction can be made how geometrical deformations, electron lone pairs, and substituent effects lead to a change in the values of ^1J(C,H) and ^2J(H,H), respectively, for hydrocarbons. © *2004 American Institute of Physics.* [DOI: 10.1063/1.1825993]

I. INTRODUCTION

The indirect isotropic spin–spin coupling constant (SSCC) J of nuclear magnetic resonance (NMR) spectroscopy represents a sensitive antenna probing the electronic structure of a molecule under the impact of a perturbation caused by the magnetic moment of the nuclei.[1–13] Therefore, SSCCs are valuable parameters to describe the electronic structure of a molecule provided one is able to decode the information contained in them. In recent work, we have developed the J-**OC**-PSP (=J-OC-OC-PSP: Decomposition of J into *o*rbital *c*ontributions using *o*rbital *c*urrents and *p*artial spin *p*olarization) method,[14,15] which provides the basis for a decomposition of the four Ramsey terms[2] of the SSCC into one-, two-, and n-orbital contributions. J-**OC**-PSP can be applied to the Fermi contact (FC),[14,15] spin dipole (SD),[16] paramagnetic spin–orbit (PSO), and the diamagnetic spin orbit (DSO) term[17,18] and its results documented by spin density, orbital current, and energy densities. This helps to understand which orbitals are particularly active to transport spin information between the coupling nuclei. Using localized molecular orbitals (LMOs) in this connection, one can study the contribution of the bond LMOs in dependence of atom electronegativity and bond polarizability,[14] the influence of lone pair LMOs on the coupling mechanism,[14] the passive but nevertheless important role of π-orbitals for spin transport,[15,18] the description of multiple bonding and π-delocalization by the noncontact terms,[19,20] or the back-tail interaction of bond LMOs in saturated molecules.[21] Also, general mechanistic features such as through-bond and through-space coupling,[21,22] multipath,[23] across-H-bond coupling,[24,25] and long range coupling[19] can be efficiently analyzed in this way.

In this work, we add a further dimension to the analysis by decomposing the spin–spin coupling mechanisms into effects taking place at the independent-electron level and effects directly related to the electron–electron interaction. Our investigation will be guided by the procedures originally designed to identify orbital polarization, delocalization, or repulsion. For example, PMO (perturbational molecular orbital) theory[26] showed that two-electron two-orbital effects are always stabilizing, which is the driving force of delocalization, hyperconjugation, anomeric effect, etc., whereas four-electron two-orbital effects are always destabilizing, which explains steric repulsion or the impossibility of getting a bond between two He atoms. The repertoire of electronic effects found by PMO theory and other MO approaches cannot be simply used to explain basic features of the spin–spin coupling mechanism. The latter involves not only zeroth-order orbitals but also first-order orbitals and, consequently, first-order densities. There is no basis to expect that what has been found for zeroth-order orbitals holds also for first-order orbitals.

We will analyze the one- and two-orbital contributions

[a)]Electronic mail: cremer@theoc.gu.se

utilizing LMOs and starting from coupled perturbed density-functional theory (CP-DFT), which we recently used to calculate all four Ramsey terms of the SSCC.[9] By using the first-order orbitals obtained with coupled perturbed theory in a form that helps to identify four basic contributions, we will be able to identify individual one- and two-electron effects and effects that are direct and those that result from a feedback of the deformed electron density on itself so that they have to be calculated in an iterative way to obtain a self-consistent description. Two of the four contributions are one-orbital terms and two two-orbital terms. We will demonstrate that spin-information is transported not only by exchange interactions but also by one-electron delocalization effects. There is both similarity and dissimilarity to the electronic effects of zeroth-order theory. Finally, we will show for two simple examples, namely the two SSCCs of methane, how the effects identified and calculated in this work can be used to understand the spin–spin coupling mechanism, to decode the information contained in the SSCCs, and to use the latter to get a better insight into the electronic structure of a molecule.

II. THEORY OF NMR SPIN–SPIN COUPLING

For the purpose of simplifying the description, we consider the coupling between two nuclei A and B, where B is the perturbing and A the responding nucleus. As orbitals we use Boys LMOs[27] because LMOs make a simple description of the spin–spin coupling mechanism possible. According to Ramsey,[2] there are three different perturbing actions, which are described by the Ramsey operators $h^{X,(B)}$ with X=FC, SD, PSO, DSO and which (with the exception of the DSO term) require the consideration of first-order orbitals in addition to the zeroth-order ones. In the following we do not consider a specific perturbation X since the formulas derived are valid for X=FC, SD, PSO equally. If the molecular electron system is perturbed by the Ramsey operator $h^{(B)}$ at nucleus B, the resulting first-order spin orbitals $|\psi_k^{(B)}\rangle$ can be expressed as a linear combination of virtual zeroth-order spin orbitals $|\varphi_a^{(0)}\rangle$ where the expansion coefficients $C_{ak}^{(B)}$ are given by relation (1)[15]

$$C_{ak}^{(B)}=\frac{1}{F_{kk}^{(0)}-\epsilon_a}\Bigg[h_{ak}^{(B)}+(\tilde{F}_k^{(B)})_{ak}+\sum_{l,l\neq k}((\tilde{F}_l^{(B)})_{ak}-F_{kl}^{(0)}C_{al}^{(B)})\Bigg]. \tag{1}$$

In Eq. (1), the $F_{kl}^{(0)}$ are the matrix elements of the zeroth-order Fock operator and ϵ_a is the orbital energy of virtual orbital $|\varphi_a^{(0)}\rangle$ where we use the symbol φ rather than ψ to indicate that in the case of the virtual orbitals canonical rather than localized spin orbitals are employed. The element $(\tilde{F}_l^{(B)})_{ak}$ is the first-order contribution to the Kohn–Sham matrix element due to the first-order change in spin orbital $|l\rangle$:

$$(\tilde{F}_l^{(B)})_{ak}=\int \mathrm{d}^3r\,\frac{\delta F_{ak}}{\delta\psi_l^{(0)}}\psi_l^{(B)}(\mathbf{r}). \tag{2}$$

The contribution to the reduced SSCC becomes then[15]

$$K^{AB}=\sum_{ak} C_{ak}^{(B)}h_{ak}^{(B)}. \tag{3}$$

The CP-DFT approach provides a complete description of the spin–spin coupling mechanism including a self-consistent adjustment of the exchange-correlation functional to the magnetic perturbation. A less accurate description is given by sum-over-states density-functional perturbation theory (SOS-DFPT),[28] which considers the exchange-correlation functional fixed in zeroth order and, accordingly, the expansion coefficient of Eq. (1) simplify to

$$C_{ak}^{(B)}=\frac{1}{F_{kk}^{(0)}-\epsilon_a}\Bigg[h_{ak}^{(B)}-\sum_{l,l\neq k}F_{kl}^{(0)}C_{al}^{(B)}\Bigg], \tag{4}$$

i.e., in SOS-DFPT just two terms determine the spin–spin coupling mechanism where in the more complete CP-DFT description four different electronic terms are responsible for the transport of spin information from perturbing to coupling nucleus.[9]

In the following, we will discuss Eqs. (1) and (4) in more detail where we could start from a general consideration since Eq. (1) was derived[15] for an arbitrary perturbation (shift in the nuclear position, electric perturbation, magnetic perturbation, etc.). However, for most of these perturbations, the Coulomb effects will play a dominant role thus leading to electronic effects quite different from those experienced in spin–spin coupling. The magnetic perturbation leading to spin–spin coupling is in so far unique as a) the exchange effects rather than Coulomb effects play the most important role and b) both one- and two-orbital effects are operative although there is no change in the total density distribution. Spin–spin coupling is not just a one-electron phenomenon as one could assume from the form of the Ramsey operators,[2,9] but involves also two-electron interactions. By taking into account the special features of magnetic perturbations, the electronic effects contributing to the spin–spin coupling mechanism can be understood in an elementary way, which shortens the discussion. For these reasons, we stick to a magnetic perturbation, indicate however explicitly generally valid features of our derivation. Generally valid are, e.g., the following considerations.

The deformation of the zeroth-order orbitals caused by a perturbation is expressed in CP-theory in terms of single excitations to virtual zeroth-order orbitals. The linear combination of these virtual orbitals will represent the first-order orbitals, which together with the zeroth-order orbitals give the deformed orbitals resulting from the perturbation. Similar as in zeroth-order theory, the first-order orbitals must fulfill certain criteria to get an optimal (stable) description of the perturbed molecular system.

(1) The orbitals must remain orthogonal to fulfill the Pauli exclusion principle (asymmetry of the molecular wave function).

(2) With the constraint (1) being obeyed, the energy calculated with the first-order orbitals must again adopt a minimum to obtain the most stable electron configuration of the molecule under the impact of the perturbation.

The changes in the orbitals according to (1) and (2) generate changes in the electron density, which are typical of a) the electronic structure of the molecule and b) the acting perturbation. Hence, one does not obtain direct information on the electronic structure, but must decode the electronic structure information always for the type of perturbation acting. This is the purpose of the present work when considering the four electronic terms of Eq. (1). We analyze them by considering conditions (1) and (2), i.e., we ask in each case how the energy is lowered and how orthogonality of the perturbed orbital is maintained.

As mentioned in the Introduction, we will carry out the analysis parallel to what we know from PMO theory, which means in each case we will also consider the zeroth-order analogue to obtain in this way an easier characterization of the electronic effects leading to the spin–spin coupling mechanism.

A. One orbital contributions: Response and self-exchange terms

In the simplest case, the transport of spin information between the two coupling nuclei comprises just one spin LMO, which interacts directly with both of the coupling nuclei. Equation (1) reveals that the one-orbital contributions comprises two parts, of which one corresponds to the direct response of the orbital to the perturbation, whereas the second one is equal to the feedback of the perturbed orbital on itself. We shall discuss the two terms in more detail for the example of the ^{1}FC(C,H) coupling in CH_4, where we assume the magnetic perturbation at H1 (perturbing nucleus). It should be emphasized that the results of this discussion are restricted neither to the FC term nor to the particular case of the C–H coupling in CH_4. However, one has to note the following difference between FC and SD terms on the one hand and the PSO term on the other hand: The FC and SD terms involve an opposite response of α and β orbitals to the perturbation, and thus a spin polarization. For the PSO term in contrast α and β orbitals change in the same way so that α and β density are kept unchanged individually. The amplitude of the orbitals remains unchanged, only their phase varies, reflecting the induced orbital current. That is there is no spin polarization in the PSO case. We will discuss the consequences of this difference below.

The perturbation gives rise to a spin polarization in the LMO σ(CH1), which is sensed by the responding nucleus C. The spin polarization of σ(CH1) corresponds to an excitation from σ(CH1) into the unoccupied orbital σ^*(CH1). We can study this process in a simple model that comprises only the orbitals σ(CH1) and the σ^*(CH1), which for brevity are denoted as spin orbitals $|l\rangle$ and $|a\rangle$, respectively. The first-order matrix element $h_{al}^{(\mathrm{H1})}$ driving the spin polarization is given by V and the energy difference $F_{aa}^{(0)}-F_{ll}^{(0)}$ as $\Delta\epsilon$. This means that we consider the total KS matrix comprising the relevant zeroth-order contributions and a (small but finite) first-order term. Consequently, we will obtain the perturbed (deformed) orbitals, consisting of the zeroth-order orbitals and a finite first-order contribution, whereas one in analytic perturbation theory would obtain the first-order orbitals as the derivatives of the perturbed orbitals with respect to the external perturbation.

If the perturbation is switched on, the orbitals respond in a way so as to reoptimize the total energy of the molecule.

1. Direct Ramsey response

The interaction energy with the external perturbation is $E_V=2C_{al}V$. It is linear in C_{al} and will describe a gain in energy if C_{al} and V have opposite signs. The excitation from $|l\rangle$ into $|a\rangle$ costs the excitation energy $E_{\mathrm{exc}}=C_{al}^2\Delta\epsilon$, which is quadratic in C_{al}. Minimizing the total energy with respect to C_{al} gives

$$C_{al}=-\frac{V}{\Delta\epsilon}, \tag{5a}$$

$$E_V=-2\frac{V^2}{\Delta\epsilon}, \tag{5b}$$

$$E_{\mathrm{exc}}=\frac{V^2}{\Delta\epsilon}, \tag{5c}$$

$$E=-\frac{V^2}{\Delta\epsilon}, \tag{5d}$$

that is, half of the gain in excitation energy has to be expended for the excitation $|l\rangle\rightarrow|a\rangle$. The Ramsey distortion takes place for each spin orbital independently. The two spin orbitals belonging to the same space orbital undergo opposite deformations, which eventually lead to equal contributions to the spin–spin coupling mechanism. Equations (5) give the energy gain for a single spin orbital. Second-order perturbation theory leads directly to Eq. (5d), however a stepwise approach to (5d) provides an insight into energy gain and loss caused by the individual processes.

2. Self-exchange contribution

The direct response term does not contain electron–electron interaction effects caused by the external perturbation. The latter become manifest by the fact that the first-order KS matrix is not constant but contains the response contribution $\tilde{F}^{(\mathrm{C})}$, which depends linearly on the excitation coefficients. In the model introduced above, this implies that $F_{al}^{(\mathrm{C})}$ no longer is constantly equal to V but gets the form $F_{al}^{(\mathrm{C})}=V+WC_{al}$ where W is a constant proportionality factor. If this is taken into account in the energy minimization, Eqs. (5) have to be modified in the way that $\Delta\epsilon$ is replaced by an effective excitation energy $\Delta\epsilon-W$. The two-electron terms thus change the effective excitation energies. More generally, the two-electron effects modify the orbital Hessian of the system.

In Eq. (1), the self-exchange contribution appears formally as the feedback of an orbital deformation on itself. Physically, this effect describes the interaction of two electrons, *viz.* the α and β electron sharing one and the same space orbital. The change of $\Delta\epsilon-W$ in the model can be comprehended in the following way: The opposite changes in the α- and β spin orbitals belonging to the same unperturbed space orbital imply that the total electron density re-

mains unchanged. The centroids of charge of the two spin LMOs will be shifted in opposite directions. This means that α- and β-electron are slightly separated from each other and that their Coulomb repulsion energy slightly decreases. The resulting extra energy gain is quadratic in the excitation (if there is no spin polarization at all, i.e., $C_{al}=0$, the orbital energy is extremal). As the total electron density (and thus the total Coulomb interaction) remains constant, this minimization of the α–β electron interaction is equivalent to a maximization of the self-interaction energy of the two electrons. This self-interaction energy appears as a part of the total exchange energy, which accounts for the notation self-exchange effect for the effect described.

The separation of α- and β-electrons influences not only the self-exchange but reduces also the correlation between the two electrons slightly. This implies an additional cost in energy, i.e., an increase of the effective $\Delta\epsilon$. This correlation effect is, however, usually much smaller than the self-exchange effect. For a general perturbation, e.g., a nuclear dislocation or an electric field, the perturbation affects also the total electron density and thus the Coulomb repulsion energy. In that case, the Coulomb effects are usually the dominating contribution of the response term.

The self-exchange mechanism takes place in essentially the same way for the SD mechanism. For the PSO mechanism, in contrast, there is no spin polarization, the only small change in the exchange potential arises from the induced orbital current. Consequently, self-exchange effects are small for the PSO term.

B. Two orbital contributions: Resonance and steric exchange interactions

As a rule, the transport of spin information involves more than one space orbital. In this case, all orbitals involved have to adjust in a way that the total energy regains its minimum (again, the two spin orbitals belonging to the same space orbital will undergo opposite changes). In distinction to the situation considered in Sec. II A, this means that an orbital can respond not only to the magnetic perturbation directly but also to the changes in another space orbital. Consequently, spin information can be transferred between the coupling nuclei along a chain of orbitals. Only the first and last orbitals in such an orbital path make an *active contribution*, i.e., interact directly with one of the nuclei, whereas the other orbitals make *passive contributions*, i.e., participate in the spin-information transport by interaction with other orbitals only. The J-**OC**-PSP method[15] allows to decompose the total SSCC into contributions from individual orbital paths at various levels of detail. In previous J-**OC**-PSP investigations, it was tacitly assumed that the transport is dominated by electron–electron interaction. However, as was mentioned in Ref. 15 and is shown in Eqs. (1) and (4), interactions between different responding orbitals are possible without any electron–electron repulsion involved. For the moment, we will call this effect *resonance interaction* (as introduced in Ref. 15) although we will later see that this term is too general and should be further specified. If one can (i) explain the nature of this *resonance interaction* and (ii) determine it quantitatively, this would allow additional insight in the spin–spin coupling mechanism and, consequently, the electronic structure of the molecules investigated.

1. Resonance interaction

At a first glance, it is surprising that transfer of spin information between two electrons can occur even if electron–electron interactions are neglected. The ultimate reason for this is the Pauli principle: The energy minimization of, e.g., orbital $|k\rangle$ is constrained by the requirement that $|k\rangle$ has to be orthogonal to all other occupied orbitals $|l\rangle$. If $|l\rangle$ responds to a perturbation then the constraints imposed on $|k\rangle$ will change, and the energy of orbital $|k\rangle$ can possibly be decreased by an appropriate deformation of $|k\rangle$.

We study the resonance interaction in more detail for a simple model system, which we derive with the ^{2}FC(H,H) coupling in CH_4 in mind. This coupling is dominated by the spin polarization of the two σ(CH) orbitals in the bond path, i.e., the most important occupied orbitals are σ(CH1) and σ(CH2), denoted by $|l\rangle$ and $|k\rangle$, and the corresponding unoccupied orbitals σ^*(CH1) and σ^*(CH2) denoted by $|a\rangle$ and $|b\rangle$ (Fig. 1). The perturbing spin is assumed at atom H1. Its dominating direct effect is to polarize spin-LMO σ(CH1), i.e., to initiate an excitation $|l\rangle \rightarrow |a\rangle$, which yields the deformed orbital $|l\rangle + c|a\rangle$ and the corresponding antibonding orbital $|a\rangle - c|l\rangle$, where c is the mixing coefficient.

For simplicity we assume that the only nonzero matrix element of the perturbing operator is $h_{al}^{(\mathrm{H1})}=V$. The orbital σ(CH2) can respond to the magnetic perturbation by a delocalization $\sigma(\mathrm{CH2}) \rightarrow \sigma^*(\mathrm{CH1})$. This leads to a change in σ(CH2), which may invoke follow-up effects such as a polarization $\sigma(\mathrm{CH2}) \rightarrow \sigma^*(\mathrm{CH2})$. The crucial effect is however the delocalization. Therefore, we exclude the virtual spin orbital $|b\rangle$ from our model and are left with the two degenerate occupied spin orbitals, whose KS matrix elements $F_{kk}^{(0)} = F_{ll}^{(0)}$ are set to zero. The Fock matrix element $F_{aa}^{(0)}$ of the virtual orbital $|a\rangle$ is given as $\Delta\epsilon$, where the Δ refers to the energy difference between k, l and $|a\rangle$. The nondiagonal KS matrix element between the two occupied orbitals $F_{kl}^{(0)}$ will be denoted t in the following. We define the two σ(CH) orbitals with the same phase, which implies $t<0$.

If t were zero, the perturbation would simply cause a polarization of σ(CH1), $C_{ak}=0$, and the result from Eq. (5) would apply. What we want to understand now is why for $t\neq 0$ it is energetically favorable that orbital $|k\rangle$ responds to the perturbation V even though orbital $|k\rangle$ is passive and not affected by V directly. As in Sec. II A, we have to determine the changes in the orbitals up to second order to obtain the individual contributions to the total energy change.

The perturbed orbitals are not determined unambiguously but only up to mutual orbital rotations. To avoid any problems resulting from this ambiguity, we use the one-particle density matrix γ rather than the perturbed orbitals. If the coefficients C_{al} and C_{ak} are given, the orthonormality requirements determine the matrix γ completely. To second order in the C_{al} and C_{ak}, one finds

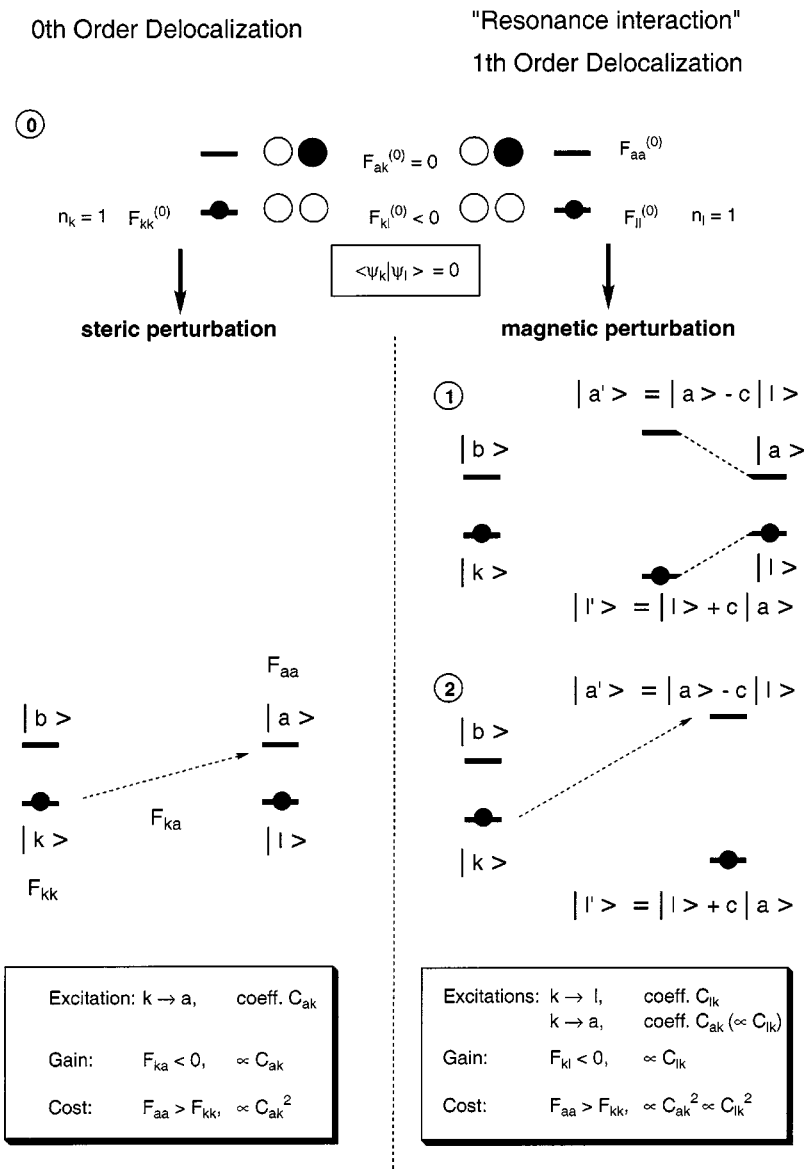

FIG. 1. Comparison of zeroth-order and first-order delocalization. A model with two fragments (two occupied and two virtual spin LMOs) is considered. In zeroth order the union of the two fragments (steric perturbation) leads to delocalization of the bonding spin LMO ψ_k into the antibonding spin orbital φ_a, which implies an energy gain proportional to coefficient C_{al} stopped at some point by the fact that orbital energy of φ_a is higher than that of ψ_k (see box on the left side). In the first order case, the magnetic perturbation leads to a deformation of spin-LMO ψ_l (step 1). The deformed orbital is then prone to accept electron density from ψ_k, i.e., a similar delocalization process (with energy gain and energy loss, see box on the right side) as in zeroth-order occurs, only that now a deformed LMO is involved. Note that the changes in the orbital energies caused by the magnetic perturbation are actually tiny.

$$\gamma_{pq}=\begin{bmatrix} 1-C_{ak}^2 & C_{ak}C_{al} & C_{ak} \\ C_{ak}C_{al} & 1-C_{al}^2 & C_{al} \\ C_{ak} & C_{al} & C_{ak}^2+C_{al}^2 \end{bmatrix}. \tag{6}$$

The perturbed KS matrix has the form

$$F_{pq}=\begin{bmatrix} 0 & t & 0 \\ t & 0 & V \\ 0 & V & \Delta\epsilon \end{bmatrix}, \tag{7}$$

and the energy of the system is

$$\begin{aligned} E&=\underbrace{2t\gamma_{kl}}+\underbrace{2V\gamma_{al}}+\underbrace{\Delta\epsilon\gamma_{aa}} \\ &=2tC_{ak}C_{al}+2VC_{al}+\Delta\epsilon(C_{ak}^2+C_{al}^2). \end{aligned} \tag{8}$$

with the matrix elements γ_{pq} as given in Eq. (6). Again, this energy is for one spin direction only. Minimizing the energy from Eq. (8) gives

$$\gamma_{kl}=-\frac{\tau}{(1-\tau^2)^2}\left(\frac{V}{\Delta\epsilon}\right)^2, \tag{9a}$$

$$\gamma_{al}=-\frac{1}{1-\tau^2}\frac{V}{\Delta\epsilon}=-\frac{V}{\Delta\epsilon}-\frac{\tau^2}{1-\tau^2}\frac{V}{\Delta\epsilon}, \tag{9b}$$

$$\gamma_{ak}=-\frac{\tau}{1-\tau^2}\frac{V}{\Delta\epsilon}, \tag{9c}$$

$$\gamma_{aa}=\frac{1+\tau^2}{(1-\tau^2)^2}\left(\frac{V}{\Delta\epsilon}\right)^2=\left(\frac{V}{\Delta\epsilon}\right)^2+\frac{\tau^2(3-\tau^2)}{(1-\tau^2)^2}\left(\frac{V}{\Delta\epsilon}\right)^2. \tag{9d}$$

Here we have introduced the parameter $\tau=t/\Delta\epsilon$, which reflects the relative strength of the interaction between the orbitals. In each term, we have separated the value for $\tau=0$ (if present) and the extra contribution arising for τ being nonzero.

The corresponding energy contributions are

$$E_{kl} = -\frac{2\tau^2}{(1-\tau^2)^2}\frac{V^2}{\Delta\epsilon}, \tag{10a}$$

$$E_{al} = -\frac{2}{1-\tau^2}\frac{V^2}{\Delta\epsilon} = -2\frac{V^2}{\Delta\epsilon} - \frac{2\tau^2}{1-\tau^2}\frac{V^2}{\Delta\epsilon}, \tag{10b}$$

$$E_{aa} = \frac{1+\tau^2}{(1-\tau^2)^2}\frac{V^2}{\Delta\epsilon} = \frac{V^2}{\Delta\epsilon} + \frac{\tau^2(3-\tau^2)}{(1-\tau^2)^2}\frac{V^2}{\Delta\epsilon}, \tag{10c}$$

leading to

$$E = -\frac{1}{1-\tau^2}\frac{V^2}{\Delta\epsilon} = -\frac{V^2}{\Delta\epsilon} - \frac{\tau^2}{1-\tau^2}\frac{V^2}{\Delta\epsilon}. \tag{11}$$

Equation (11) indicates that the coupling between $|k\rangle$ and $|l\rangle$ decreases the total energy. From Eqs. (10a) and (10b) it becomes evident that this decrease results from the changes in the matrix elements γ_{al} and γ_{kl}. Inspection of Eq. (9) shows that γ_{kl} is of order τ whereas the change in γ_{al} is of order τ^2. This indicates that the $k \leftrightarrow l$ coupling in first instance causes a change in γ_{kl}, i.e., a $|k\rangle \rightarrow |l\rangle$ delocalization, which is energetically favorable because of $t<0$. This change feeds then back into orbital $|l\rangle$ and increases the $|l\rangle \rightarrow |k\rangle$ excitation, which is favorable because of V. In detail, the scenario of the resonance interaction is as follows (see Fig. 1):

(1) The perturbation V causes a $|l\rangle \rightarrow |a\rangle$ excitation according to Eq. (11). The occupied orbital $|l\rangle$ is changed into $|l'\rangle = |l\rangle + c|a\rangle$, the virtual orbital $|a\rangle$ into $|a'\rangle = |a\rangle - c|l\rangle$ with a small coefficient c. (Note that this process does not affect the orthonormality of the orbitals.)
(2) The matrix element of $F^{(0)}$ between $|a'\rangle$ and $|k\rangle$ is nonzero. This drives a delocalization of the electron in orbital $|k\rangle$ into the new virtual orbital $|a'\rangle$;
(3) This, in turn, modifies $|k\rangle$ and $|b\rangle$, and the matrix element between $|l'\rangle$ and the modified virtual orbital $|b'\rangle$ becomes nonzero, which results in a delocalization $|l'\rangle \rightarrow |b'\rangle$. (This process is not shown in Fig. 1).

Actually, steps 2 and 3 proceed not one by one but in form of a mutual feedback.

It should be noticed that the perturbation V is rather small. It is in the order of $\alpha^2\kappa$ a.u., where $\alpha = 1/137.04$ is Sommerfeld's fine structure constant and $\kappa = 1/1816$ is the ratio of electron and proton mass, hence $V \approx 10^{-7}$ a.u. The shifts in the orbital energies are negligible compared to the energy difference $\Delta\epsilon$, i.e., we can consider $\Delta\epsilon$ as constant.

Eventually, the energy gain initiating the response of orbital $|k\rangle$ is the delocalization $|k\rangle \rightarrow |l\rangle$ that is contained in the delocalization $|k\rangle \rightarrow |a'\rangle$ in step 2. Equation (9a) shows that this effect is of second order in the one-particle density matrix, and its impact on the total energy is measured by a part of the zero-order KS matrix, viz. t. In conventional perturbation theory, a second-order effect would not be considered, and the corresponding energy gain would be absorbed by the term $C_{al}V$. The energy cost limiting the interaction is the population of $|a'\rangle$ by excitation from the $|k\rangle$ orbital (step 2).

The feedback between steps 2 and 3 shows that the resonance interaction gives rise to different kinds of effects:

(a) Orbital $|k\rangle$ reacts to the perturbation even though there is no direct interaction with the perturbation V. This effect is essential for the spin transport along chains of two or more orbitals;
(b) orbital $|l\rangle$ reacts not only to the perturbation V. In addition, there is a "recoil" from orbital $|k\rangle$ to orbital $|l\rangle$. One finds that this *echo effect*[15] enhances the response of orbital $|l\rangle$ to the external perturbation.

In general, both orbitals $|k\rangle$ and $|l\rangle$ couple directly to the perturbing nucleus. For the purpose of modeling this case, we modify the model in Fig. 1 in the way that the perturbing nucleus is the central C atom. In this case, the dominating unoccupied orbital is no longer of σ^*(CH1) character but an a_1-symmetrical orbital that may be formed from both from a $3s$(C1) (Rydberg) orbital and a symmetric combination of the four σ^*(CH) orbitals. The perturbing matrix elements are $h_{al}^{(C)}$ and $h_{ak}^{(C)}$, which we will denote as V and V', respectively. Although $V' = V$, we keep different notations to distinguish between the effects of V and V'. Equations (9b) and (9c) get then the form

$$\gamma_{al} = -\frac{V}{\Delta\epsilon} - \frac{\tau^2}{1-\tau^2}\frac{V}{\Delta\epsilon} - \frac{\tau}{1-\tau^2}\frac{V'}{\Delta\epsilon}, \tag{12}$$

where the expression for γ_{ak} is found by interchanging V and V'. Again, γ_{al} contains the direct impact of the perturbation V and the echo contribution V [see (b) above]. In addition, there is a term proportional to V'. This term, which is analogous to the term containing γ_{ak} in Eq. (9c), describes processes where the perturbation acts on orbital $|l\rangle$, which in turn acts on $|k\rangle$. This kind of contribution will be called *external orbital contribution*: An external orbital (i.e., an orbital that is not in the bond path between the two nuclei) passes spin information from the perturbing nucleus to an orbital in the bond path. (We note in this connection that the external one-orbital contributions, e.g., those of σ(CH2), σ(CH3), and σ(CH4) in methane, in addition, pass spin information directly to the responding nucleus.) Hence, we can distinguish between three resonance contributions: (a) a spin-transport resonance effect involving an active orbital l and a passive orbital k; (b) an echo resonance effect again involving an active orbital l and a passive orbital k; (c) an external orbital resonance effect involving an active orbital l and another active orbital k.

The resonance interaction is closely connected to the Pauli principle, which is relevant only for electrons with equal spin. Therefore, resonance interaction takes place between electrons with equal spin in different space orbitals.

The resonance interaction shows analogies to zeroth-order delocalization processes. This is demonstrated in the left part of Fig. 1: Describing, for example, a conjugated π system such as 1,3-butadiene by the interaction of two ethene units, the Fock matrix element between the π_1 (π_2) orbital and the π_2^* (π_1^*) orbital of the second (first) ethene unit is negative, i.e., a delocalization $\pi_1 \rightarrow \pi_2^*$ ($\pi_2 \rightarrow \pi_1^*$) provides an energy gain, which is linear in the amplitude of the delocalization. However, as the π^* orbitals are higher in energy than the π orbitals, there is an energy cost proportional to the square of the amplitude, which limits the degree

of delocalization to a finite value. In the model system considered, the situation is similar as soon as the perturbation V has caused an excitation $|l\rangle \rightarrow |a\rangle$. Then, the virtual orbital is a superposition of $|l\rangle$ and $|a\rangle$. That is, an excitation from $|k\rangle$ into this new virtual orbital gives both an energy gain due to $t<0$ and an energy loss because of $\Delta\epsilon>0$. Again, the gain and the loss are linear and quadratic in the delocalization amplitude, respectively.

The comparison reveals that the resonance effect corresponds to a delocalization effect in zeroth order involving now a deformed orbital, i.e., it is better to speak of a *first-order delocalization effect* rather than a resonance effect, which is normally associated with a superposition of state functions rather than orbitals (although the term resonance is often used in a more general way).

2. Calculation of the first-order delocalization effect

Actually, it will be impossible to separate the direct response of the orbitals to the external potential (caused, e.g., by a magnetic perturbation) from first order delocalization (resonance effect) if canonical molecular orbitals (CMOs) are used. CMOs are special in so far as their orbital energy is stationary with regard to any small deformation of an individual orbital. Consequently, their deformation under the impact of an external potential leads right away to an adjustment of their delocalization tails. This also implies that for CMOs small changes of one orbital have no impact on the orthogonality constraints of the other CMOs. Instead, the consequences of the Pauli principle are integrated in the forms of the orbitals: The CMOs are delocalized and this implies that there is no need for a mutually dependent reoptimization.

In the case of LMOs, stationary character is given only for the whole set of occupied orbitals. Therefore, any change in an occupied LMO because of an external perturbation requires also first-order delocalization effects in the set of occupied LMOs and provides the possibility to separate direct response and first-order delocalization. This is one of the advantages of using LMOs. CMOs can be considered as orbitals that artificially enclose the first-order delocalization interaction into the one-orbital response terms.

3. Steric exchange interaction

Contrary to the one-electron two-orbital delocalization effect (note that spin orbitals are considered), the steric exchange effect is a genuine two-electron two-orbital process that is driven by the exchange interaction between the electrons. This interaction is reflected by the fact that the first-order KS matrix elements contain not only the bare perturbation $h^{(\mathrm{H1})}$ but in addition a response part $\tilde{F}$ that depends on the first-order orbitals.

Using the same model as for the discussion of the first-order delocalization interaction, the steric exchange proceeds then in the following steps (see Fig. 2; H1 perturbing nucleus):

1. The perturbation causes a spin polarization in the bond CH1, i.e., an excitation $|l\rangle \rightarrow |a\rangle$. The orbitals $|l\rangle$ and $|a\rangle$ are transformed into $|l\rangle + c|a\rangle$ and $|a\rangle - c|l\rangle$, respectively. (Again, this polarization does not affect the orthogonality of the orbitals.)

2. The induced spin polarization leads to an extra term $\tilde{F}^{(\mathrm{H1})}$ in the exchange potential. This potential is α-attractive and β-repulsive in regions with α surplus spin density and vice versa in regions with β surplus spin density. Depending on the shape and mutual position of the orbitals, $\tilde{F}^{(\mathrm{H1})}$ may have nonvanishing matrix elements for all pairs of occupied and unoccupied orbitals. The matrix elements al and bl give rise to an additional polarization and delocalization of orbital $|l\rangle$ (see above). The matrix elements ak and bk drive delocalization and polarization effects of orbital $|k\rangle$, and the orbital $|k\rangle$ can mix with both $|a\rangle$ and $|b\rangle$. This process is the central part of the steric exchange interaction. The situation is slightly different from that for the first-order delocalization interaction: In the latter case, the delocalization $|k\rangle \rightarrow |a'\rangle$ was the essential response to the deformation of $|l\rangle$, whereas for the steric-exchange interaction it depends on the matrix elements of $\tilde{F}^{(\mathrm{H1})}$, i.e., eventually on the shape and mutual arrangement of the occupied and unoccupied orbitals involved whether polarization or delocalization (or both) dominate the response of orbital $|k\rangle$. The energy gain for the steric exchange interaction arises from an optimization of the equal-spin overlap between orbitals $|k\rangle$ and $|l\rangle$, which is favorable to maximize the exchange energy. The cost in energy is again given by the population of the unoccupied orbitals.

3. The response of orbital $|k\rangle$, too, generates an additional exchange potential, which gives rise to further responses in orbitals $|k\rangle$ and $|l\rangle$.

Analogously as for the resonance interaction, processes 2. and 3. proceed in mutual feedback until the energetically optimal state is reached.

The steric exchange interaction attempts to maximize the spin polarization in the system: A surplus of α density attracts additional α density from other orbitals and vice versa. The same is true for the self-exchange interaction, as was shown in Sec. II A. Both effects together maximize the separation of α and β electrons in the molecule and minimize thus their mutual repulsion. That is, the steric exchange interaction is driven by electrons with opposite spin that reside in different space orbitals. They should thus be seen not as two individual physical processes but as two aspects of one and the same process. This is in line with the facts that self-interaction energy and Fermi exchange in a molecule are described on an equal footing and that their separation is not unambiguous but depends on the choice of orbitals (see Refs. 29 and 30). Consequently, the separation of the total exchange interaction into self-exchange and steric exchange contributions also depends on the choice of orbitals whereas their sum is invariant in this respect. A natural choice is to use LMOs to maximize the self-exchange part.[29,30] In this way, LMOs are more suitable to separate the two effects than CMOs.

Similarly as the self-exchange interaction, the steric-exchange interaction is small for the PSO term.

A counterpart of the steric exchange interaction in classical chemistry is the steric repulsion occurring as two frag-

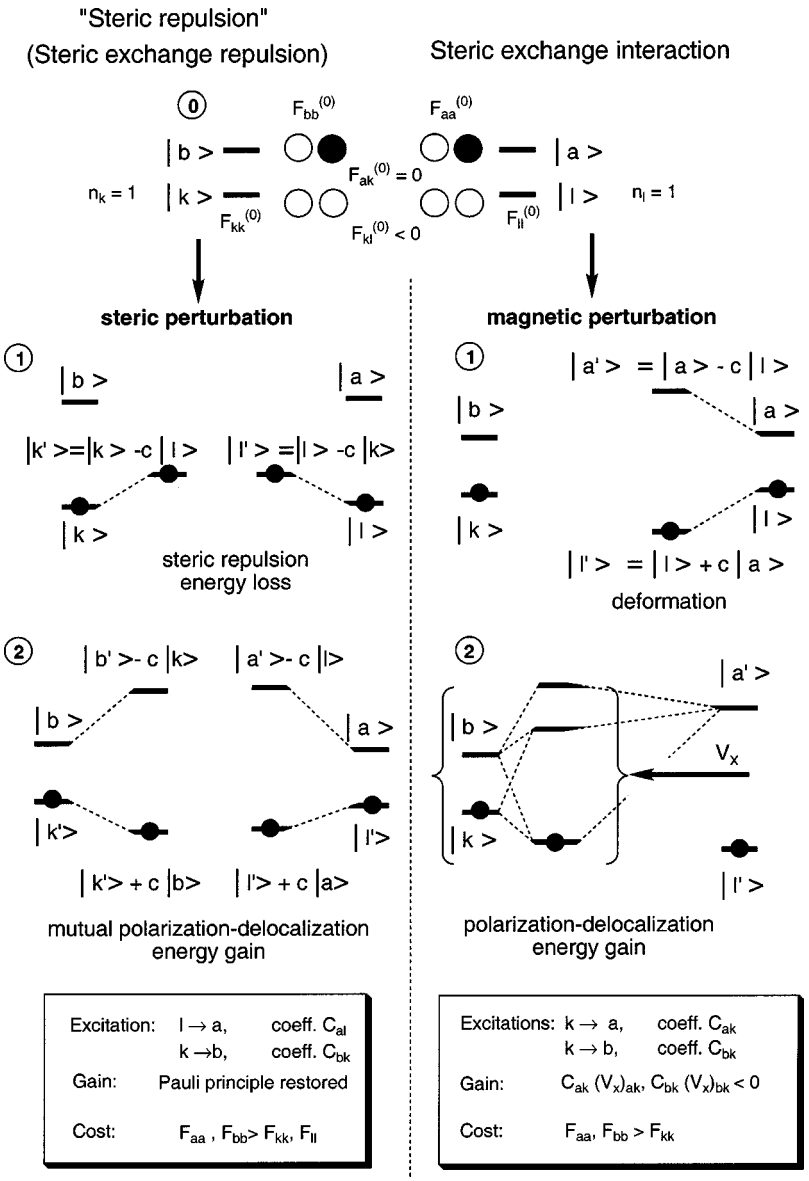

FIG. 2. Comparison of zeroth-order steric repulsion and first-order steric exchange interaction. A model with two fragments (two occupied and two virtual spin LMOs) is considered. In zeroth order the union of the two fragments (steric perturbation, step 1) leads to an energy loss due steric repulsion, which in the second step is slightly compensated by orbital polarization and restoring of the orthogonality of the orbitals. In the first-order case, there is again a deformation of spin-LMO ψ_l due to the magnetic perturbation (step 1). Spin-LMO ψ_k, can interact then with its own antibonding orbital (polarization) or the deformed antibonding of ψ_l (delocalization), which leads in any case to an energy gain. Note that the changes in the orbital energies caused by the magnetic perturbation are actually tiny.

ments (atoms or molecules) approach each other. The situation is shown in the left part of Fig. 2: For the fragments being separated, the occupied orbitals do not overlap and are thus orthogonal. Also, the Coulomb interaction between the fragments is small as attractive and repulsive contributions compensate each other.

For decreasing distance between the fragments (steric perturbation), two changes take place in the system that imply a cost in energy and thus counteract the mutual approach:

1. The two LMOs get mutual orthogonalization tails to obey the Pauli principle, i.e., the new LMOs $|k'\rangle = |k\rangle - c|l\rangle$ and $|l'\rangle = |l\rangle - c|k\rangle$ are formed. The orthogonalization tails make the fragment LMOs partly antibonding, and their kinetic energy is higher than that of the original orbitals.

2. Both repolarizations $|k\rangle \rightarrow |b\rangle$, $|l\rangle \rightarrow |a\rangle$ and delocalizations $|k\rangle \rightarrow |a\rangle$, $|l\rangle \rightarrow |b\rangle$ may decrease the overlap between the deformed orbitals $|k'\rangle$ and $|l'\rangle$ and thus counteract the increase in kinetic energy. The energy gain through these excitations is linear in the amplitudes, the cost (due to the population of the virtual orbitals) quadratic.

There are important differences between the steric-exchange interaction occurring in spin–spin coupling and the steric repulsion. The main reason is that the steric repulsion is driven by the overlap between equal-spin occupied LMOs and does not depend on the electron–electron repulsion. Indeed, both the mutual orthogonalization in step 1 and the excitations in step 2 will affect both the total Coulomb and the exchange interaction, but none of the two steps is driven by these two-electron energy contributions. The steric exchange interaction in the spin–spin coupling, in contrast, is caused by a reoptimization of the electron–electron interaction energy.

C. Calculation of the spin–spin coupling terms

The J-**OC**-PSP method[14,15] makes it possible to analyze the spin–spin coupling mechanism by decomposing the total SSCC into contributions from individual orbitals and orbital paths. A further extension of J-**OC**-PSP is provided by splitting the orbital contributions into their one-electron (i.e., di-

rect Ramsey response and first order delocalization) and electron–electron interaction (i.e., self-exchange and steric-exchange) parts.

Equation (1) formally provides a separation of the total SSCC into the four different contributions. However, a direct use of Eq. (1) by calculating, e.g., the first-order delocalization interaction directly from the last term in (1) is not possible: This term contains the expansion coefficients $C_{al}^{(B)}$, which in CP-DFT are calculated with self-exchange and steric exchange interactions included and thus a mixing of the various parts occurs. The different mechanisms can be separated if the SSCC calculation are carried out once at the CP-DFT level and once at the SOS-DFPT level. SOS-DFPT calculations consume little CPU time, so they mean no relevant extra cost. The equation for the SOS-DFPT orbital expansion coefficients is given in Eq. (4) in implicit form. An equivalent explicit expression is

$$C_{ak}^{\mathrm{SOS}}=\sum_{k',a'}(\mathrm{H}_0^{-1})_{ak,a'k'}h_{a'k'}^{(B)}, \tag{13}$$

where H_0 is the zeroth-order Hessian matrix

$$(H_0)_{ak,a'k'}=(\epsilon_a\delta_{kk'}-F_{kk'}^{(0)})\,\delta_{aa'}. \tag{14}$$

For canonical virtual orbitals, the inversion of H_0 can be easily performed by diagonalizing H_0 in the indices k, l separately for each value of $|a\rangle$.

In a J-**OC**-PSP analysis, sets of *orbital-selected calculations* are done for a given SSCC, where selected sets of orbitals are partly or fully excluded from the spin-transfer mechanism.[15] The contribution of a given orbital or a group of orbitals is then found as the difference of the SSCC for a calculation where this orbital (group) is incorporated and a second calculation where it is not. By combining selected-orbital calculations appropriately, individual orbital contributions can be isolated in a specific form, as is shown in detail in Ref. 15. The separation can be done at two basic levels of J-**OC**-PSP theory:[14,15] At J-**OC**-PSP1,[14] the orbitals to be excluded are set passive, i.e., their interaction with the perturbation operators $h^{(A)}$, $h^{(B)}$ is set to zero, whereas their interaction with other orbitals is retained. J-**OC**-PSP1 provides a decomposition of the total SSCC with respect to the active orbital contributions, i.e., with respect to the first and last orbitals in each orbital path. A complete analysis of individual orbital paths, including the passive orbitals in the interior of the path, is given by the J-**OC**-PSP2 approach,[15] where the eliminated orbitals are frozen (their interaction both with the $h^{(A)}$, $h^{(B)}$ and with the other orbitals is suppressed).

The decomposition of each J-**OC**-PSP orbital contribution into the four one-electron and electron interaction parts can then be done in the following way:

(1) All selected-orbital calculations for the J-**OC**-PSP analysis are done both with SOS-DFPT and with CP-DFT;
(2) the J-**OC**-PSP orbital contributions are determined both for the CP-DFT and the SOS-DFPT results;
(3) the J-**OC**-PSP terms obtained at the SOS-DFPT level are the one-electron contributions. The difference of a J-**OC**-PSP term for CP-DFT and its SOS-DFPT counterpart provides the electron-interaction part of the component.

The only remaining question is how to perform the orbital selected SSCC calculations. For J-**OC**-PSP1, this is accomplished by replacing $h^{(A)}$, $h^{(B)}$ by the orbital-selected operators

$$h_{ak}^{(N),\mathrm{sel}}=\sum_{a'k'}(\delta_{aa'}\delta_{kk'}-P_{ak,a'k'}^{\mathrm{sel}})h_{a'k'}^{(N)} \quad (N=A,B), \tag{15a}$$

$$P_{ak,a'k'}^{\mathrm{sel}}=\begin{cases}1 & \text{for } a=a',k=k',k \text{ passive}\\ 0 & \text{otherwise}\end{cases}. \tag{15b}$$

For J-**OC**-PSP2, $h^{(A)}$ and $h^{(B)}$ are replaced in the same way where the projection operator P from Eq. (15b) accounts for all orbitals that should be frozen. In addition, one has to suppress the interactions between the frozen and the remaining orbitals by the following modification of the Hessian:

$$(H_0^{\mathrm{sel}})_{ak,a'k'}=\sum_{a''k''}\sum_{a'''k'''}P_{ak,a''k''}^{\mathrm{sel}}(H_0)_{a''k'',a'''k'''}P_{a'''k''',a'k'}^{\mathrm{sel}}. \tag{16}$$

Technically, this implies that all elements $F_{kl}^{(0)}$ that contain one or two frozen orbitals are set to zero.

We will illustrate the J-**OC**-PSP decomposition for the ^{1}FC(C,H1) coupling term in CH_4, where we assume that C is the perturbing nucleus. The SSCC contribution of LMO σ(CH1) is determined from a calculation where σ(CH1) is kept active whereas all other σ(CH) orbitals are kept frozen (the 1s orbital is kept active in all calculations):

$$K^{\mathrm{dir},[\sigma(\mathrm{CH1})]}=K^{\mathrm{SOS}}[\mathrm{a,f,f,f}], \tag{17a}$$

$$K^{\text{self-X},[\sigma(\mathrm{CH1})]}=K^{\mathrm{CP}}[\mathrm{a,f,f,f}]-K^{\mathrm{SOS}}[\mathrm{a,f,f,f}]. \tag{17b}$$

Here, the superscripts dir and self-X stand for direct Ramsey distortion and self-exchange interaction, respectively. For two- or more-orbital contributions, one has analogously a decomposition into first-order delocalization and steric-exchange terms, which will be denoted with the indices deloc and steric, respectively. The notation [a,f,f,f] denotes the active (a) LMO σ(CH1) and the frozen (f) LMOs σ(CH2), σ(CH3), σ(CH4). Analogously, the contribution from each of the external σ(CH) orbitals is

$$K^{[\sigma(\mathrm{CH2})]}=K[\mathrm{f,a,f,f}]. \tag{18}$$

Here and in the following, we suppress the decomposition into (dir) and (self-X) or (deloc) and (steric) contributions for the sake of brevity. If we start from the orbital selection in Eq. (17) and additionally set LMO σ(CH2) passive, the resulting SSCC contains the one-orbital contribution from σ(CH1) and the echo effect from σ(CH2) on σ(CH1). Hence, the echo contribution from σ(CH2) on σ(CH1) can be determined as

$$K^{[\sigma(\mathrm{CH1})\leftrightarrow\sigma(\mathrm{CH2})]}=K[\mathrm{a,p,f,f}]-K[\mathrm{a,f,f,f}]. \tag{19}$$

This example shows that it may be meaningful to combine features from J-**OC**-PSP1 and J-**OC**-PSP2 and to perform calculations where some orbitals are passive while others are kept frozen.

If σ(CH2) is active rather than passive, we will get two additional contributions compared to Eq. (19): First, the external orbital contribution $\sigma(\mathrm{CH2})\rightarrow\sigma(\mathrm{CH1})$; second, the one-orbital contribution from σ(CH2). The external orbital contribution from the path $\sigma(\mathrm{CH2})\rightarrow\sigma(\mathrm{CH1})$ is, therefore,

$$K^{[\sigma(\mathrm{CH1})\leftarrow\sigma(\mathrm{CH2})]}=K[\mathrm{a,a,f,f}]-K[\mathrm{a,p,f,f}]-K[\mathrm{f,a,f,f}]. \tag{20}$$

There are more higher-order contributions, for instance, the interaction between σ(CH2) and σ(CH3) may influence the echo and external-bond contributions of these orbitals on σ(CH1), etc. However, these contributions are small.

The SSCCs are linear in the expansion coefficients of the first-order orbitals. This means that one can decompose the coefficients C_{al} in the same way as the SSCCs K, e.g., in analogy to Eq. (17)

$$C^{\mathrm{dir}}_{a,[\sigma(\mathrm{CH1})]}=C^{\mathrm{SOS}}_{a,\sigma(\mathrm{CH1})}[\mathrm{a,f,f,f}], \tag{21a}$$

$$C^{\text{self-X}}_{a,[\sigma(\mathrm{CH1})]}=C^{\mathrm{CP}}_{a,\sigma(\mathrm{CH1})}[\mathrm{a,f,f,f}]-C^{\mathrm{SOS}}_{a,\sigma(\mathrm{CH1})}[\mathrm{a,f,f,f}]. \tag{21b}$$

Accordingly, one can decompose the changes of the orbitals into contributions from the different one- and two-electron mechanisms. We note that the subscript $[\sigma(\mathrm{CH1})]$ at the left hand side of Eqs. (21a) and (21b) serves two purposes: It specifies both the LMO to which the expansion coefficient refers, i.e., σ(CH1), and the contribution in question, i.e., the one-orbital contribution. Analogously, the notation $[\sigma(\mathrm{CH1})\leftarrow\sigma(\mathrm{CH2})]$ denotes the external orbital contribution from σ(CH2) to σ(CH1) etc.

In previous publications,[14–19] we have demonstrated that a graphical representation of the first-order orbitals as well as the corresponding first-order densities is of great help to see relationships between spin–spin coupling and features of the electronic structure. The J-**OC**-PSP contributions to C_{al} can thus be used not only to calculate the corresponding contributions to the SSCC but also to graphically represent the effect of the individual nucleus-electron and electron–electron interaction effects on both the first-order orbitals and the first-order densities. In the present paper, this is done for the first time, which proves particularly useful to comprehend the mechanism of the first order delocalization interaction. For that purpose, the first-order orbitals are determined from Eq. (21) according to

$$\varphi^{\mathrm{dir}}_{[\sigma(\mathrm{CH1})]}(\mathbf{r})=\sum_a C^{\mathrm{dir}}_{a,[\sigma(\mathrm{CH1})]}\varphi^{(0)}_a(\mathbf{r}). \tag{22}$$

We give this equation exemplary for one particular contribution, the generalization to other contributions and orbitals is straightforward. The contribution of this orbital to the first-order spin density is then obtained as

$$m^{\mathrm{dir}}_{[\sigma(\mathrm{CH1})]}(\mathbf{r})=4\varphi^{\mathrm{dir}}_{[\sigma(\mathrm{CH1})]}(\mathbf{r})\varphi^{(0)}_{\sigma(\mathrm{CH1})}(\mathbf{r}). \tag{23}$$

We calculated the SSCC and its J-**OC**-PSP components for CH_4 at the B3LYP[31–33] level of theory, using the $(11s,7p,2s/6s,2p)/[7s,6p,2d/4s,2p]$ basis set.[34,35] The geometry of the molecule was optimized at the B3LYP/6-31G(d,p) level.[36] For the calculation of the SSCCs with CP-DFT and SOS-DFPT, the algorithm described by us previously[9] was used. Boys' LMOs were calculated as described in Ref. 14. The FC spin density distributions, zeroth order, and first order LMOs will be shown in form of contour line diagrams, where the contour levels are given by a geometric progression with the ratio of $100^{1/5}$ between two subsequent contours. All calculations as well as the graphical representation of the results were done with the program package COLOGNE 04.[37]

III. A SIMPLE APPLICATION EXAMPLE: SPIN–SPIN COUPLING IN METHANE

There are two SSCC is methane, the one-bond SSCC $^1J(^{13}\mathrm{C},^1\mathrm{H})=^1J(\mathrm{C,H})$ and the two-bond SSCC $^2J(^1\mathrm{H},^1\mathrm{H})=^2J(\mathrm{H,H})$, which have values of 125[38] and −12.4 Hz.[39] The calculations carried out in this work lead to 124.3 and −11.1 Hz in good agreement with experiment where one has to consider vibrational corrections of 5.0 and −0.7 Hz.[40] The quantum chemical description chosen should provide reasonable Ramsey terms and orbital contributions thus providing the basis for a meaningful decomposition of the SSCC. In both cases the FC term (122.8 and −11.6 Hz) dominates the other Ramsey contributions and, therefore, we can focus on the FC term in the analysis (although the derivation presented in Sec. II is applicable to all Ramsey terms). It has to be noted that the SOS-DFPT description of the SSCCs of methane yields 70.1 and −0.2 Hz which underlines the necessity of including a self-consistent adjustment of the perturbed orbitals to the changes in the exchange potential.

A. The one-bond SSCC ^1J(C,H)

The perturbing nucleus is C and H1 is the responding nucleus both indicated in Fig. 3 by black balls. Figure 3 gives a summary of the calculations performed (CP-DFT and SOS-DFPT calculations 1a to 1e) and the J-**OC**-PSP results obtained (results in the framed box). For the purpose of identifying the active bond LMO considered the corresponding CH bond is given as a bold line. Similarly, passive LMOs are denoted by normal lines whereas frozen LMOs are given as dashed lines. For each orbital, the direct contribution (Ramsey response, first order delocalization contribution) and the self-consistent contribution (self-exchange, steric exchange) is given.

The FC term of the one-bond SSCC ^1J(C,H) is dominated by the contribution of the bond LMO. The Ramsey response term is 94 Hz, which is enhanced by the one-orbital self-exchange part by another 70 Hz (Fig. 3). All other orbital contributions involve the external CH bond LMOs and lead to a reduction of the Ramsey distortion term from 164 to 123 Hz (by 25%). Six external contributions are significant: Each external orbital is distorted by the magnetic perturbation and can transfer spin information from perturbing to responding nucleus via its tail. This leads to a Ramsey response of $3\times-4.07=-12.2$ Hz enhanced by a self-exchange contribution of $3\times-1.05=-3.2$ Hz totalling −15.3 Hz.

There are also negative two-orbital contributions involving the external orbitals where the larger ones are all negative. Most important is the two-orbital first-order delocalization interaction of totally −19.6 Hz complemented by a steric exchange term of −4.7 Hz. Why is the majority of the contributions involving an external orbital negative? This is

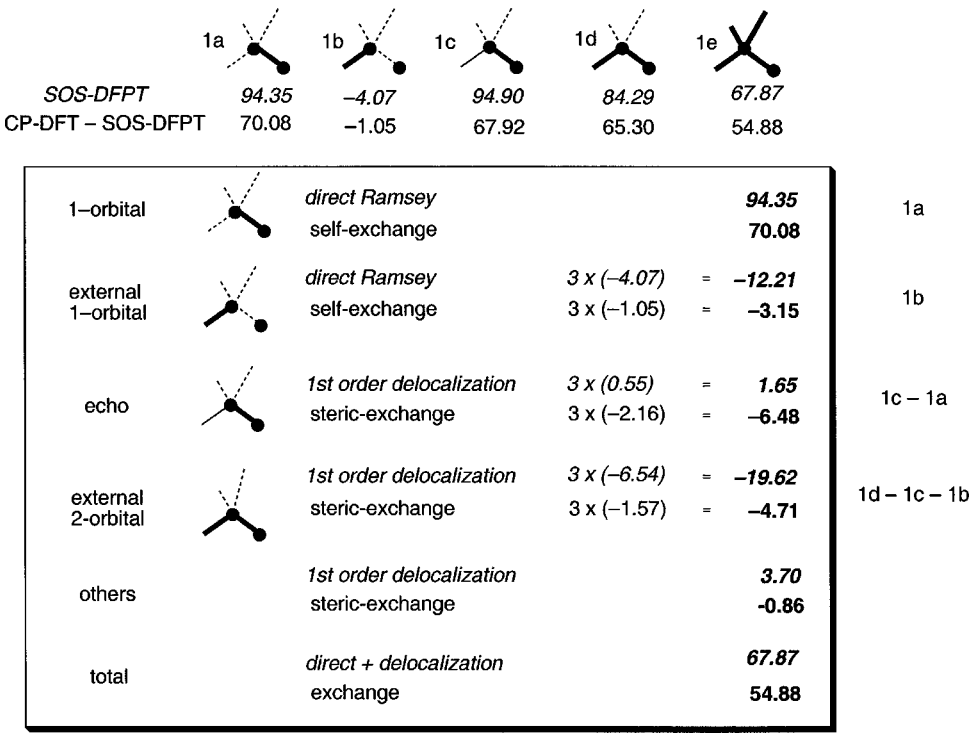

FIG. 3. J-OC-PSP decomposition of the SSCC ^1J(C,H) of methane. Outside the box the results of the SOS-DFPT and CP-DFT calculations needed are given. Inside the box, the most important basic contributions to the SSCC are listed. All values in Hz.

explained in Figs. 4–6, which give the zeroth-order bond LMOs σ(CH1) and σ(CH2) (Fig. 4), the first-order orbital σ(CH1) parts corresponding to one of the four electronic FC coupling effects (Fig. 5), and finally the equivalent FC spin density distributions (Fig. 6).

In each case, the perturbing nucleus is assumed to possess α spin, which implies that due to Fermi coupling the surrounding spin density is negative (preference of β spin). This holds for the total FC spin density and most of the partial FC spin densities where in the latter case the spin density close to the perturbing nucleus is not necessarily always negative. Independent of this the FC spin density at the responding nucleus always defines the sign of the corresponding FC contribution (α surplus: positive; β surplus: negative).

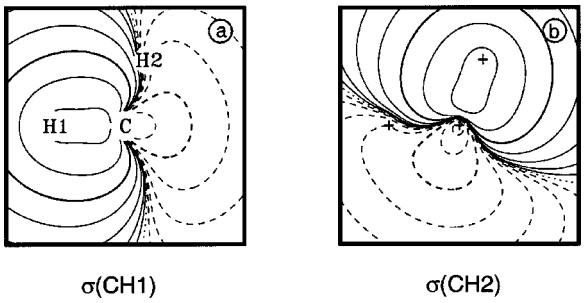

FIG. 4. Contour line diagrams of the methane LMOs σ(CH1) (a) and σ(CH2) (b) shown in the plane of the three nuclei C, H1, and H2. The contour lines are chosen in geometric progression with a factor of $100^{1/5}$ between neighboring lines. Solid lines indicate positive amplitudes, dashed lines negative amplitudes, dotted lines the zero contour. The contour levels 0.1 and 10 are marked by bold contour lines. In Fig. (b), the nuclear positions are given just by crosses.

The partial FC spin densities reveal that the (internal) one-orbital terms are positive [Figs. 6(a) and 6(b)], the external one-orbital terms (not shown) negative, and the external two orbital terms [with the exception of the echo delocalization term, Fig. 6(c)] negative [Figs. 6(d)–6(f)]. Since the sign of the FC spin density at the responding nucleus (here H1) is given by the product of the signs of zeroth- [positive, Fig. 4(a)] and first-order σ(CH1) LMO amplitude, the analysis of the FC spin densities can be carried out with the help of the first-order orbital contributions (Fig. 5). The first order orbital contributions, which are just under the impact of the perturbing nucleus C1, must possess a_1-symmetry. These are the first-order orbital contribution resulting from the direct Ramsey response [Fig. 5(a)], the echo delocalization contribution [Fig. 5(c)], and the two active orbital first-order delocalization contribution [Fig. 5(e)].

The first-order orbital contribution of the self-exchange part [Fig. 1(b)] seems also to possess a_1 symmetry, however, closer inspection reveals a slight asymmetry, which is simply a result of the self-interaction of the σ(CH1) orbital. The FC spin density of σ(CH1) [see Fig. 6(a)] acts on the first-order orbital shown in Fig. 5(a) to give the first-order orbital of Fig. 5(b). Since the FC spin density of σ(CH1) is very large at C (not shown) thus enhancing the perturbation potential of C, the self-exchange first-order orbital keeps its a_1-symmetrical form close to the C nucleus and changes only farther away.

The form of the first-order orbitals of Fig. 5 can be derived using the formulas of Sec. II. The first and the second term in Eq. (9b) correspond to the orbital contributions shown in Figs. 5(a) and 5(b), respectively, whereas Eq. (9c) relates to the external orbital delocalization effect [Fig. 5(e)].

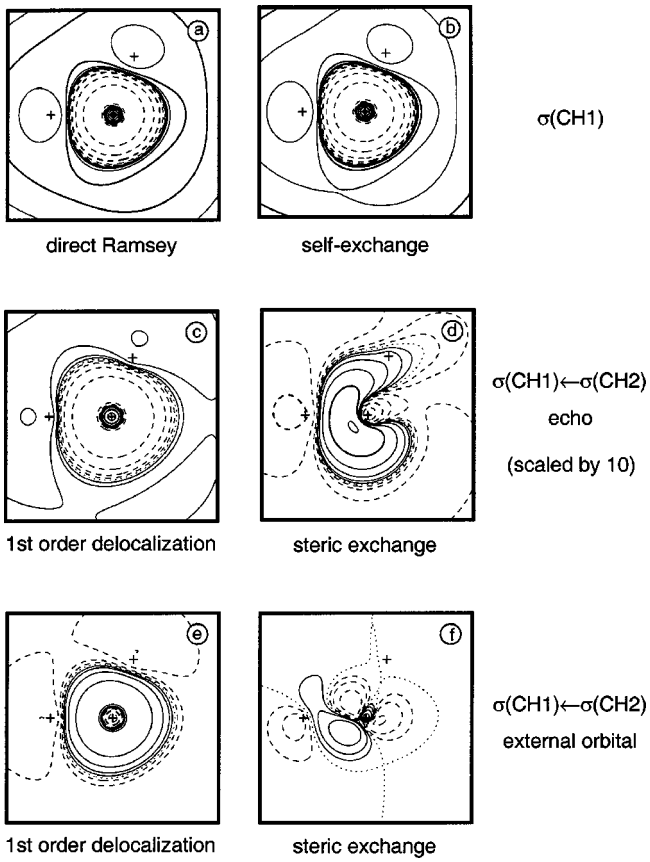

FIG. 5. Contour line diagrams of the first-order orbitals needed for the analysis of the SSCC ^1J(C,H) of methane shown in the plane of the three nuclei C, H1, and H2 [indicated by crosses, compare with Fig. 4(a)]. The perturbed nucleus is C (α spin assumed). The contour lines are chosen in geometric progression with a factor of $100^{1/5}$ between neighboring lines. Solid lines indicate positive amplitudes, dashed lines negative amplitudes, dotted lines the zero contour. The contour levels 0.1 and 10 are marked by bold contour lines. (a) $\varphi^{\mathrm{dir}}_{[\sigma(\mathrm{CH1})]}(\mathbf{r})$ (b) $\varphi^{\text{self-X}}_{[\sigma(\mathrm{CH1})]}(\mathbf{r})$ (c) $\varphi^{\mathrm{deloc}}_{[\sigma(\mathrm{CH1})\leftarrow\sigma(\mathrm{CH2})]}(\mathbf{r})$, scaled by a factor of 10. (d) $\varphi^{\mathrm{steric}}_{[\sigma(\mathrm{CH1})\leftarrow\sigma(\mathrm{CH2})]}(\mathbf{r})$, scaled by a factor of 10. (e) $\varphi^{\mathrm{deloc}}_{[\sigma(\mathrm{CH1})\leftrightarrow\sigma(\mathrm{CH2})]}(\mathbf{r})$ (f) $\varphi^{\mathrm{steric}}_{[\sigma(\mathrm{CH1})\leftrightarrow\sigma(\mathrm{CH2})]}(\mathbf{r})$.

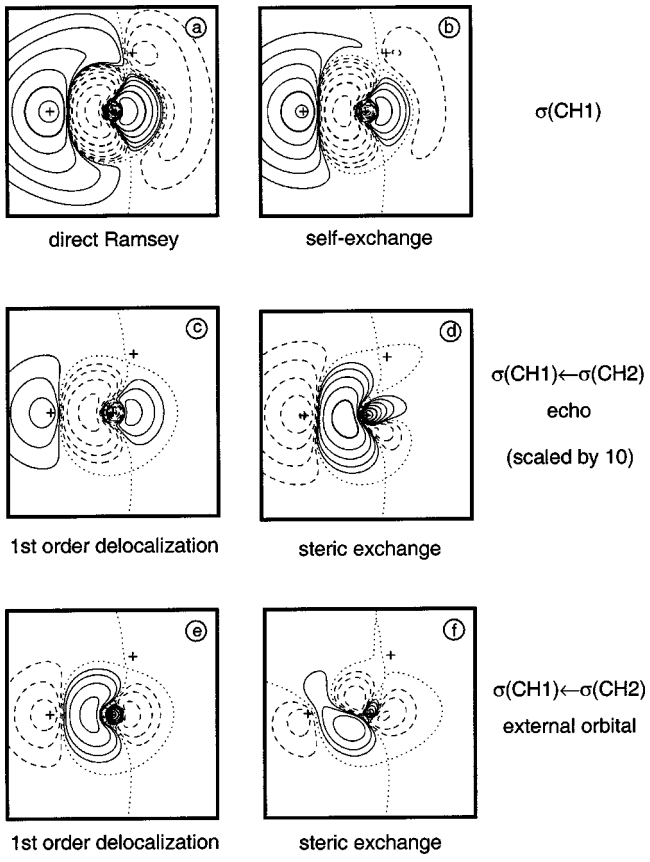

FIG. 6. Contour line diagrams of the FC spin densities needed for the analysis of SSCC ^1J(C,H) of methane shown in the plane of the three nuclei C, H1, and H2 [indicated by crosses, compare with Fig. 4(a)]. The perturbed nucleus is C (α spin assumed). The contour lines are chosen in geometric progression with a factor of $100^{1/5}$ between neighboring lines. Solid lines indicate a dominance of α spin density, dashed contour lines β spin density, and dotted contour represent the zero contour of the FC spin density. The contour levels 0.1 and 10 are marked by bold contour lines. (a) $m^{\mathrm{dir}}_{[\sigma(\mathrm{CH1})]}(\mathbf{r})$ (b) $m^{\text{self-X}}_{[\sigma(\mathrm{CH1})]}(\mathbf{r})$ (c) $m^{\mathrm{deloc}}_{[\sigma(\mathrm{CH1})\leftarrow\sigma(\mathrm{CH2})]}(\mathbf{r})$, scaled by a factor of 10. (d) $m^{\mathrm{steric}}_{[\sigma(\mathrm{CH1})\leftarrow\sigma(\mathrm{CH2})]}(\mathbf{r})$, scaled by a factor of 10. (e) $m^{\mathrm{deloc}}_{[\sigma(\mathrm{CH1})\leftrightarrow\sigma(\mathrm{CH2})]}(\mathbf{r})$ (f) $m^{\mathrm{steric}}_{[\sigma(\mathrm{CH1})\leftrightarrow\sigma(\mathrm{CH2})]}(\mathbf{r})$.

As revealed by Eqs. (9), the direct response does not depend on the interaction element ($\tau = t/\Delta\epsilon$), the external orbital delocalization effect depends on $-\tau$, and the echo delocalization effect on τ^2 (where one should consider that τ is a qualitative measure for the overlap between $|k\rangle$ and $|l\rangle$). There are two possible virtual orbitals of a_1 symmetry, which have to be considered: The all antibonding $3a_1$ orbital with nodal surfaces close to the H nuclei and the Rydberg $3s$ orbital with the first nodal sphere close to the C nucleus. These two virtual orbital determine the general shape of the first order orbitals in Figs. 5(a), 5(c), and 5(e). For example, close to the nucleus the 3s contribution is visible. A stronger dependence on the interaction element $\tau = t/\Delta\epsilon$ increases the weight of the lower lying $3a_1$ virtual orbital and the nodal surfaces are shifted closer to the H nuclei, which in turn reduces the corresponding contribution. In this way, Fig. 5 reveals why the resulting FC contributions decrease from Fig. 5(a) (94.4) to Fig. 5(e) (−19.6) and Fig. 5(c) (1.7 Hz, Fig. 3). Equation (9d) shows also that the external orbital delocalization effect depends on $-\tau$ with $\tau < 0$ so that the corresponding first orbital part experiences a sign inversion thus leading to a negative FC contribution of −19.6 Hz.

If the perturbed σ(CH2) orbital acts on σ(CH1) [Figs. 5(d) and 5(f)] there is no longer any symmetry. Decisive for the magnitude of the FC partial contribution is how close the nodal plane of the corresponding first-order orbital is shifted toward the responding nucleus (the closer, the smaller the magnitude of the contribution).

B. The two-bond SSCC ^2J(H,H)

In Fig. 7, the results of the decomposition of SSCC ^2J(H1,H2) (perturbation at H1) are summarized. There is only one important contribution, which is the two-orbital, two-electron steric exchange interaction of −10.5 Hz. This term will change just by −0.7 Hz if the sum of all other (partly positive, partly negative) contributions (Fig. 7) is added.

In Fig. 8, the first-order orbitals relating to the one-orbital contributions and the two-orbital delocalization and steric exchange term are shown whereas in Fig. 9, the corresponding FC spin density distributions are displayed. These

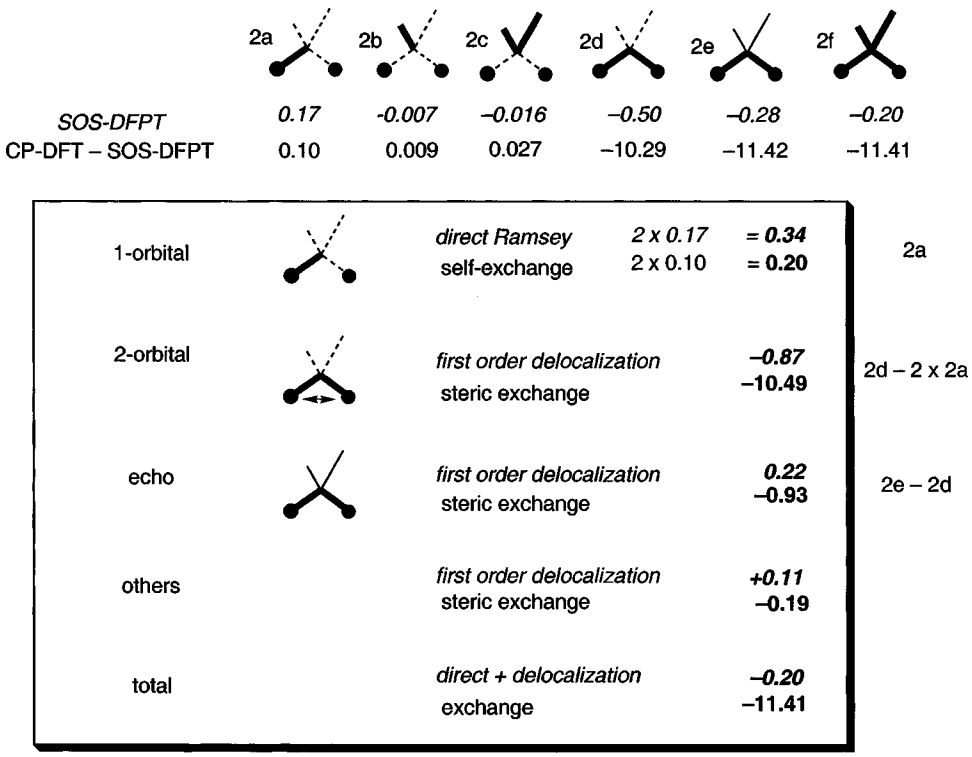

FIG. 7. J-**OC**-PSP decomposition of the SSCC ^2J(H,H) of methane. Outside the box the results of the SOS-DFPT and CP-DFT calculations needed are given. Inside the box, the most important basic contributions to the SSCC are listed. All values in Hz.

Figures directly reveal that the one-orbital contributions must be all small because the responding (and/or perturbing) nucleus is always located close to the nodal surface of both the zeroth-order LMO [Fig. 4(a): H2; Fig. 4(b): H1] and the first-order orbital [Figs. 8(a)–8(d): H2] so that there is only little FC spin density at the responding nucleus in these cases [Figs. 9(a)–9(d)].

Why is for the two-orbital interaction term of ^{2}FC(H,H) the delocalization interaction negligible? For both ^{2}FC(H,H) and ^{1}FC(C,H) the orbital path is the same. In the former case, the magnetic perturbation at H1 leads to a σ(CH1)$\rightarrow\sigma^*$(CH1) excitation, which in turn causes an excitation from σ(CH2) into σ^*(CH1), i.e., a delocalization of σ(CH2). This, however, is less efficient for the FC coupling mechanism since the σ^*(CH1) orbital has a nodal surface close to H2, so that the resulting spin density at H2 is close to zero.

The magnitude and sign of the two-orbital steric exchange term σ(CH1)$\rightarrow\sigma$(CH2) can be explained with the help of Figs. 8(f) and 9(f). As discussed above this term can transport spin information either by delocalization or polarization of σ(CH2). Delocalization into σ^*(CH1) would produce a first-order orbital similar to that shown in Fig. 8(e). Hence, the deviation from this first-order orbital indicates the influence of polarization, which leads to an increased contribution of σ(CH2). The nodal surface, which is close to H2 in Fig. 8(e) is shifted to the right in Fig. 8(f) and a more negative steric exchange contribution (-10.5 Hz, Fig. 7) results.

The different two-orbital contributions found for ^{2}FC(H,H) and ^{1}FC(C,H) are a result of symmetry connected with the different bond paths. In the case of ^{1}FC(C,H), the perturbing C nucleus does not change the symmetry of the molecular wave function and accordingly implies a_1 symmetry of the first-order orbitals (provided no other perturbation comes in). An admixture of the 3*s* Rydberg orbital (suppressed as explained for the echo effect) leads to a sizable first-order delocalization contribution. In the case of ^{2}FC(H,H), the perturbing nucleus lowers the symmetry and accordingly both σ^*(CH1) (for delocalization) and σ^*(CH2) (for polarization) can participate in the first-order orbitals. Figure 8(f) shows that the delocalization is the dominating effect as regards the overall deformation of the orbital, however, the polarization plays an important role with respect to the spin–spin coupling in that it moves away the nodal plane of the first-order orbital from the responding nucleus.

We can conclude that the geminal proton–proton coupling in methane is essentially a two-electron exchange interaction effect transporting spin polarization from H1 to H2. All other contributions are small because of the nodal structure of the orbitals involved.

IV. CHEMICAL RELEVANCE OF THE J-OC-PSP ANALYSIS

In this work, we have demonstrated that spin–spin coupling involves one-electron as well as two-electron effects where the latter are exchange driven. Among the one-electron effects one has to consider the Ramsey response effects (distortion caused by the magnetic perturbation) and the first order delocalization (''resonance'') effect. First order delocalization is responsible for spin-information transport, a finding that was not taken into account sufficiently in previ-

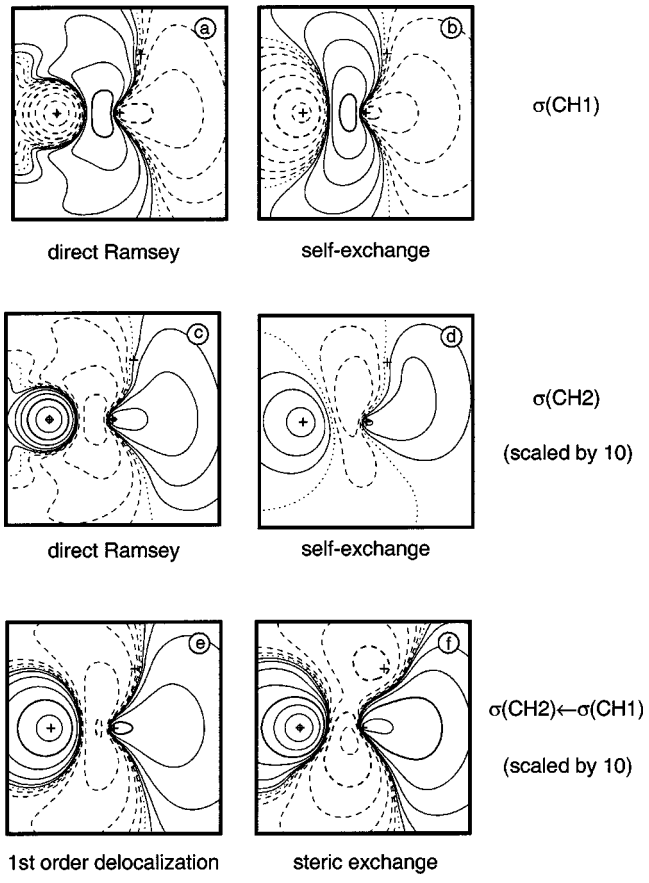

FIG. 8. Contour line diagrams of the first-order orbitals needed for the analysis of the SSCC ^1J(C,H) of methane shown in the plane of the three nuclei C, H1, and H2 [indicated by crosses, compare with Fig. 4(a)]. The perturbed nucleus is H1 (α spin assumed). The contour lines are chosen in geometric progression with a factor of $100^{1/5}$ between neighboring lines. Solid lines indicate positive amplitudes, dashed lines negative amplitudes, dotted lines the zero contour. The contour levels 0.1 and 10 are marked by bold contour lines. (a) $\varphi^{\mathrm{dir}}_{[\sigma(\mathrm{CH1})]}(\mathbf{r})$ (b) $\varphi^{\mathrm{self\text{-}X}}_{[\sigma(\mathrm{CH1})]}(\mathbf{r})$ (c) $\varphi^{\mathrm{dir}}_{[\sigma(\mathrm{CH2})]}(\mathbf{r})$, scaled by a factor of 10. (d) $\varphi^{\mathrm{self\text{-}X}}_{[\sigma(\mathrm{CH2})]}(\mathbf{r})$, scaled by a factor of 10. (e) $\varphi^{\mathrm{deloc}}_{[\sigma(\mathrm{CH2})\leftarrow\sigma(\mathrm{CH1})]}(\mathbf{r})$, scaled by a factor of 10. (f) $\varphi^{\mathrm{steric}}_{[\sigma(\mathrm{CH2})\leftarrow\sigma(\mathrm{CH1})]}(\mathbf{r})$, scaled by a factor of 10.

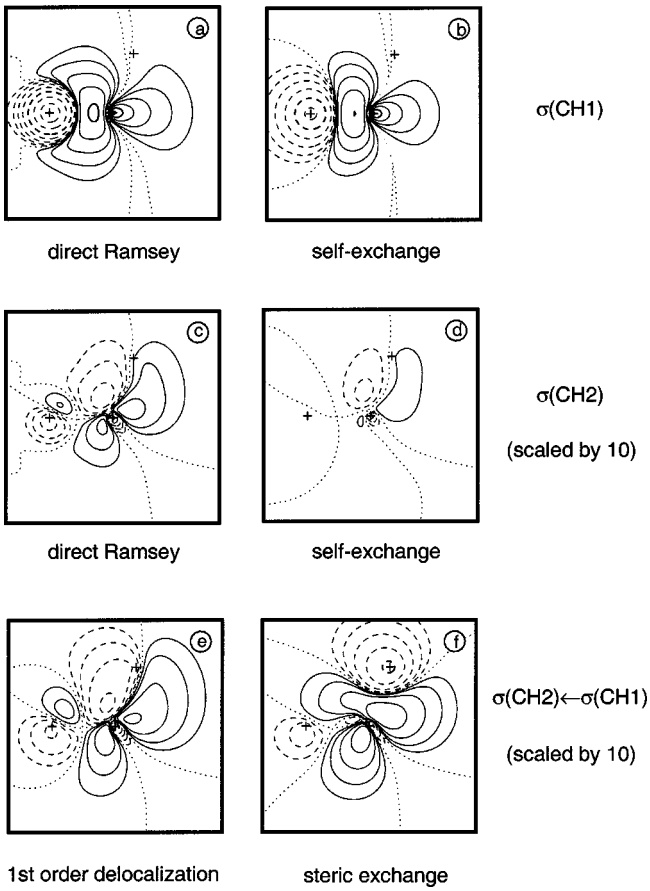

FIG. 9. Contour line diagrams of the FC spin densities needed for the analysis of the SSCC ^1J(C,H) of methane shown in the plane of the three nuclei C, H1, and H2 [indicated by crosses, compare with Fig. 4(a)]. The perturbed nucleus is H1 (α spin assumed). The contour lines are chosen in geometric progression with a factor of $100^{1/5}$ between neighboring lines. Solid lines indicate a dominance of α spin density, dashed contour lines β spin density, and dotted contour represent the zero contour of the FC spin density. The contour levels 0.1 and 10 are marked by bold contour lines. (a) $m^{\mathrm{dir}}_{[\sigma(\mathrm{CH1})]}(\mathbf{r})$ (b) $m^{\mathrm{self\text{-}X}}_{[\sigma(\mathrm{CH1})]}(\mathbf{r})$ (c) $m^{\mathrm{dir}}_{[\sigma(\mathrm{CH2})]}(\mathbf{r})$, scaled by a factor of 10. (d) $m^{\mathrm{self\text{-}X}}_{[\sigma(\mathrm{CH2})]}(\mathbf{r})$, scaled by a factor of 10. (e) $m^{\mathrm{deloc}}_{[\sigma(\mathrm{CH2})\leftarrow\sigma(\mathrm{CH1})]}(\mathbf{r})$, scaled by a factor of 10. (f) $m^{\mathrm{steric}}_{[\sigma(\mathrm{CH2})\leftarrow\sigma(\mathrm{CH1})]}(\mathbf{r})$, scaled by a factor of 10.

ous investigations. By identifying the basic electronic effects that carry the FC spin–spin coupling mechanism (for a summary, see Table I) a number of important conclusions can be drawn:

1) There are some basic differences between the two-orbital electronic effects of zeroth- and first-order orbital theory where of course in the latter case always the nature of the perturbation has to be considered (here a magnetic perturbation, which leads to a dominance of exchange effects). The zeroth-order and first-order delocalization effects are similar. They involve in the latter case just deformed orbitals, however, in both cases an energy gain is produced combined in the case of the first order orbitals also with a transport of spin information. The two-orbital interaction effects (steric repulsion and steric exchange interaction) are different although they both involve deformed orbitals (Fig. 2). Since, however, they are dominated by different interacting potentials (V_J and V_X), the consequences of the two effects are different: In the first case, an energy loss results by electron repulsion whereas in the second case orbital repolarization and delocalization guarantees an energy gain needed for transport of spin information.

2) Each electronic term identified in connection with the spin–spin coupling mechanism relates to other molecular properties such as symmetry, electronegativity of the constituting atoms, bond polarizability, the energy and nodal properties of low-lying excited orbitals, etc. Analysis of the various effects provides in this way a detailed insight into the electronic structure. a) Direct Ramsey response and self exchange are related to the electronegativity of the coupling nuclei and the bond pair polarizability. For example, a large electronegativity leads to a tight bond orbital and a large self-exchange effect. A large bond polarizability implies a larger direct Ramsey response. First order delocalization tests for low-lying unoccupied orbitals as does also the steric exchange effect. In the case of echo and external first-order delocalization, we have derived in this work simple formulas to qualitatively estimate the magnitude of these effects (see Table I).

3) Symmetry considerations are useful to determine the

TABLE I. Basic electronic effects acting in the NMR spin–spin coupling mechanism.[a]

Term	SSCC ^{n}J	Orbitals: space-LMOs	Electrons	Calculation	Method	Changes
Ramsey response	1, 2, *n*	one active *l*	one	direct	SOS	$-V/\Delta\epsilon$
Self-exchange	1, 2, *n*	one active *l*	two	self-consist.	CP—SOS	
First order delocalization	1, 2, *n*	two	one	direct	SOS	
spin transport	2, *n*	active *l* + active *k*	one	direct	SOS	
	3, *n*	active *l*,*k* + passive *m*	one	direct	SOS	
echo	1, 2, *n*	active *l* + passive *k*	one	direct	SOS	$-V\tau/\Delta\epsilon$
external orbital	1, 2, *n*	active *l* + active *k*	one	direct	SOS	$-V\tau^2/\Delta\epsilon$
Steric exchange interaction	1, 2, *n*	two	two	self-consist.	CP—SOS	
spin transport	2, *n*	active *l* + active *k*	two	self-consist.	CP—SOS	
	3, *n*	active *l*,*k* + passive *m*	two	self-consist.	CP—SOS	
echo	1, 2, *n*	active *l* + passive *k*	two	self-consist.	CP—SOS	
external orbital	1, 2, *n*	active *l* + active *k*	two	self-consist.	CP—SOS	

[a]The interaction element $\tau = t/\Delta\epsilon$ is smaller than zero.

selection rules for the various terms. This has been demonstrated by placing the perturbing nucleus into the symmetry center and excluding in this way all virtual orbitals in the discussion of the direct terms that are not totally symmetric. In the case of the size-consistent terms, the spin density of the perturbing orbital helps to predict the magnitude of the electron interaction terms.

Using the analysis worked out, the SSCCs of methane can be easily decomposed and analyzed:

4) The FC spin–spin coupling mechanism of a one-bond SSCC is basically different from that for a two-bond SSCC. In the first case the one-orbital Ramsey contribution amplified by the self-exchange term dominates where external orbital contributions, especially first-order delocalization. diminish the one-orbital contributions by 20%–30%. In the second case the two-orbital steric exchange term is responsible for coupling; Ramsey and first-order delocalization contribution do not play any significant role.

The insight into the spin–spin coupling mechanism in methane gained by the J-**OC**-PSP analysis, makes it possible to predict changes in the SSCC caused by geometrical changes and substituent effects.

5) Predicted influences for one-bond SSCC ^1J(C,H) in hydrocarbons: All influences should concern primarily the bond LMO effect, however, changes in the external orbital effects must not be overlooked because of their non-negligible magnitude.

5a) The atomic numbers of the coupling nuclei are decisive for the magnitude of the bond-orbital FC terms, however, they will always be positive. With increasing electronegativity of the nuclei the self-exchange term will increase whereas high atomic numbers and small electronegativity differences lead to increased polarizabilities and larger Ramsey response terms.

5b) Electronegative substituents will have a similar effect on the self-exchange terms than an increase in the bond polarity caused by a given electronegativity difference, i.e., the ^1J(C,H) becomes larger. This is experimentally confirmed.[38] However, electronegative substituents will also shift the nodal surface between C and H1 toward the C nucleus thus leading to more negative external orbital contributions. *A priori*, it is not clear whether the bond orbital and external orbital contributions change in the same ratio so that the SSCC just depends on the electronegativity of the substituent. SSCC measurements for substituted methane suggest that this is the case.[38]

5c) Electron lone pairs can be considered as special substituents. They should lead to a especially strong negative external orbital effect similar to that of an electropositive substituent. The SSCC ^1J(X,H) should decrease strongly. This was confirmed for SSCC ^1J(X,H) of XH_n molecules.[14] With increasing number of lone pairs SSCC ^1J(X,H) becomes negative.

6) Predicted influences for geminal SSCC ^2J(H,H) in hydrocarbons: Influences can be particularly easily predicted because one can concentrate largely on the steric exchange effect [Fig. 8(f)].

6a) By widening the HCH angle, the responding nucleus moves toward the nodal surface on the right side of the first-order orbital [compare with Fig. 8(f)], passes it, then enters the region with a positive amplitude of the first-order orbital and continues in the direction of an increasing positive amplitude. This means that angle widening changes the SSCC from −12.4 to 0 and then to positive values. Exactly, this is found in the series methane (−12.4), bicyclo[2.1.1]hexane, bicyclobutane unit (−5.4), cyclopropane (−4.3), ethene (2.5 Hz).[39]

6b) Electronegative substituents increase the repolarization included in the steric exchange effect. In this way, the nodal surface on the right of H2 [Fig. 8(f)] moves away from the responding nucleus. The ^2J(H,H) value keeps its negative sign but becomes larger in magnitude. The reverse effect can be expected for electropositive substituents. These substituents effects have also been observed for SSCCs ^2J(H,H).[39]

6c) A similar effect as that for electronegative substituents can be expected if the HCH group can interact with unsaturated group (π-bond) via hyperconjugation. The SSCC ^2J(H,H) becomes more positive.[39]

The results of this work lead also to two important general conclusions. (i) It is a typical approach to correlate measured one-bond or two-bond SSCCs with the electronegativity of substituents, delocalization parameters or geometrical quantities. The analysis carried out in this work reveals that in the case of one-bond SSCCs the success of such an approach is questionable since different environmental effects

(geometry, substituents) can lead to different changes in the coupling mechanism that are not necessarily proportional to a single quantity such as a bond angle or an electronegativity parameter. For example, a substituent can increase the one-orbital bond contribution, however, increase also significantly the magnitude of the (negative) external orbital effect so that the total effect is small despite a large electronegativity of the substituent. Hence, useful correlation with environmental parameters can only be obtained if the SSCC is decomposed in a J-**OC**-PSP analysis and individual contributions are used for the relationship with other quantities.

(ii) In the literature, there have been various attempts to relate one-bond SSCC to bond properties.[41] The present work reveals that this an ill-based attempt because of the influence of the external orbital effects. If one wants to correlate SSCCs with other bond properties one has to consider first, whether the properties under consideration are strongly or less strongly environment dependent. For example, the bond length is less sensitive with regard to the environment whereas the SSCC is very sensitive. Accordingly, these two properties do not correlate unless one freezes largely the environment [correlation of ^1J(C,C) values in benzenoid aromatics[42]] or one excludes all environmental effects via the J-**OC**-PSP analysis and use only the one-orbital Ramsey distortions for the correlation. Work is in progress to test this hypothesis.

ACKNOWLEDGMENTS

Calculations were done on the supercomputers of the Nationellt Superdatorcentrum (NSC), Linköping, Sweden. D.C. thanks the NSC for a generous allotment of computer time. J.G. thanks Carl Tryggers Stiftelse for financial support.

[1] See, e.g., *Encyclopedia of Nuclear Magnetic Resonance*, edited by D. M. Grant and R. K. Harris (Wiley, Chichester, UK, 1996), Vols. 1–8, and references cited therein.
[2] N. F. Ramsey, Phys. Rev. **91**, 303 (1953).
[3] J. Kowalewski, Prog. Nucl. Magn. Reson. Spectrosc. **11**, 1 (1977); J. Kowalewski, Annu. Rep. NMR Spectrosc. **12**, 81 (1982).
[4] For reviews, see T. Helgaker, M. Jaszunski, and K. Ruud, Chem. Rev. (Washington, D.C.) **99**, 293 (1998); H. Fukui, Prog. Nucl. Magn. Reson. Spectrosc. **35**, 267 (1999).
[5] J. Oddershede, in *Methods in Computational Molecular Physics*, edited by S. Wilson and G. H. F. Diercksen (Plenum, New York, 1992), p. 303; R. D. Wigglesworth, W. T. Raynes, S. P. A. Sauer, and J. Oddershede, Mol. Phys. **92**, 77 (1997); **94**, 851 (1998); T. Enevoldsen, J. Oddershede, and S. P. A. Sauer, Theor. Chem. Acc. **100**, 275 (1998); R. D. Wigglesworth, W. T. Raynes, S. Kirpekar, J. Oddershede, and S. P. A. Sauer, J. Chem. Phys. **112**, 3735 (2000).
[6] A. Laaksonen, J. Kowalewski, and V. R. Saunders, Chem. Phys. **80**, 221 (1983); O. Vahtras, H. Ågren, P. Jørgensen, H. J. Aa. Jensen, T. Helgaker, and J. Olsen, J. Chem. Phys. **96**, 2118 (1992); **97**, 9178 (1992).
[7] S. A. Perera, M. Nooijen, and R. J. Bartlett, J. Chem. Phys. **104**, 3290 (1996).
[8] J. Gauss and J. F. Stanton, Chem. Phys. Lett. **276**, 70 (1997); A. A. Auer and J. Gauss, J. Chem. Phys. **115**, 1619 (2001).
[9] V. Sychrovský, J. Gräfenstein, and D. Cremer, J. Chem. Phys. **113**, 3530 (2000).
[10] For independent CP-DFT developments, see T. Helgaker, M. Watson, and N. C. Handy, J. Chem. Phys. **113**, 9402 (2000); V. Barone, J. E. Peralta, R. H. Contreras, and J. P. Snyder, J. Phys. Chem. A **23**, 5607 (2002); J. E. Peralta, V. Barone, M. C. de Azua, and R. H. Contreras, Mol. Phys. **99**, 655 (2001); J. E. Peralta, M. C. de Azua, and R. H. Contreras, Theor. Chem. Acc. **105**, 165 (2000).
[11] R. H. Contreras and J. C. Facelli, Annu. Rep. NMR Spectrosc. **27**, 255 (1993).
[12] R. H. Contreras and J. E. Peralta, Prog. Nucl. Magn. Reson. Spectrosc. **37**, 321 (2000); R. H. Contreras, J. E. Peralta, C. G. Biribet, M. C. Ruiz De Azua, and J. C. Faceli, Annu. Rep. NMR Spectrosc. **41**, 55 (2000).
[13] R. H. Contreras, V. Barone, J. C. Facelli, and J. Peralta, Annu. Rep. NMR Spectrosc. **51**, 167 (2003).
[14] A. Wu, J. Gräfenstein, and D. Cremer, J. Phys. Chem. **107**, 7043 (2003).
[15] J. Gräfenstein, T. Tuttle, and D. Cremer, J. Chem. Phys. **120**, 9952 (2004).
[16] J. Gräfenstein and D. Cremer, Chem. Phys. Lett. **387**, 415 (2004).
[17] J. Gräfenstein and D. Cremer, Chem. Phys. Lett. **383**, 332 (2004).
[18] J. Gräfenstein, E. Kraka, and D. Cremer, J. Phys. Chem. A **108**, 4520 (2004).
[19] J. Gräfenstein, T. Tuttle, and D. Cremer, Phys.Chem.Chem.Phys. (to be published).
[20] D. Cremer, E. Kraka, A. Wu, and W. Lüttke, Chem. Phys. Chem. **5**, 349 (2004).
[21] J. Gräfenstein and D. Cremer, Mag. Reson. Chem. **42**, 5138 (2004).
[22] J. Gräfenstein and D. Cremer, J. Am. Chem. Soc. (to be published).
[23] A. Wu and D. Cremer, Phys. Chem. Chem. Phys. **5**, 4541 (2003); J. Gräfenstein and D. Cremer, J. Phys. Chem. (to be published).
[24] T. Tuttle, E. Kraka, A. Wu, and D. Cremer, J. Am. Chem. Soc. **126**, 5093 (2004).
[25] T. Tuttle, J. Gräfenstein, A. Wu, E. Kraka, and D. Cremer, J. Phys. Chem. B **108**, 1115 (2004).
[26] M. J. S. Dewar and R. C. Dougherty, *The PMO Theory of Organic Chemistry* (Plenum, New York, 1975); T. A. Albright, J. K. Burdett, and M. H. Whangbo, *Orbital Interactions in Chemistry* (Wiley, New York, 1985).
[27] S. F. Boys, Rev. Mod. Phys. **32**, 296 (1960).
[28] V. G. Malkin, O. L. Malkina, and D. R. Salahub, Chem. Phys. Lett. **221**, 91 (1994); V. G. Malkin, O. L. Malkina, M. E. Casida, and D. R. Salahub, J. Am. Chem. Soc. **116**, 5898 (1994); O. L. Malkina, D. R. Salahub, and V. G. Malkin, J. Chem. Phys. **105**, 8793 (1996); R. M. Dickson and T. Ziegler, J. Phys. Chem. **100**, 5286 (1996); P. Bouř and M. Buděšínský, J. Chem. Phys. **110**, 2836 (1999).
[29] V. Polo, J. Gräfenstein, E. Kraka, and D. Cremer, Chem. Phys. Lett. **352**, 469 (2002); V. Polo, J. Gräfenstein, E. Kraka, and D. Cremer, Theor. Chem. Acc. **109**, 22 (2003).
[30] J. Gräfenstein, E. Kraka, and D. Cremer, J. Chem. Phys. **120**, 524 (2004); J. Gräfenstein, E. Kraka, and D. Cremer, Phys.Chem.Chem.Phys. **6**, 1096 (2004).
[31] A. D. Becke, Phys. Rev. A **38**, 3098 (1988).
[32] C. Lee, W. Yang, and R. P. Parr, Phys. Rev. B **37**, 785 (1988).
[33] A. D. Becke, J. Chem. Phys. **98**, 5648 (1993).
[34] S. Huzinaga, *Approximate Atomic Wave Functions* (University of Alberta Press, Edmonton AB, Canada, 1971).
[35] W. Kutzelnigg, U. Fleischer, and M. Schindler, in *NMR—Basic Principles and Progress* (Springer, Heidelberg, 1990), Vol. 23, p. 165.
[36] P. C. Hariharan and J. A. Pople, Theor. Chim. Acta **28**, 213 (1973).
[37] E. Kraka, J. Gräfenstein, M. Filatov *et al.*, COLOGNE 2004, Göteborg University, Göteborg, 2004.
[38] H. O. Kalinowski, S. Berger, and S. Braun, *^{13}C-NMR-Spektroskopie* (Georg Thieme Verlag Stuttgart, 1984), and references cited therein.
[39] H. Günther, *NMR-Spectroscopy* (Thieme, New York, 1983).
[40] P. O. Åstrand, K. Ruud, K. Mikkelsen, and T. Helgaker, J. Chem. Phys. **110**, 9463 (1999); A. T. Ruden, O. B. Lutnes, T. Helgaker, and K. Ruud, *ibid.* **118**, 9572 (2003).
[41] K. Kamienska-Trela, Spectrochim. Acta, Part A **36**, 239 (1980).
[42] D. Cremer and H. Günther, Liebigs Ann. Chem. **763**, 87 (1972); see also Ref. 39 and the citations given therein.